

# NUMERICAL MODELING OF NONIDEAL DETONATIONS IN AMMONIUM NITRATE/ALUMINIUM MIXTURES AND THEIR BLAST EFFECT

Khasainov B.A. and Ermolaev B.S.

N. Semenov Institute of Chemical Physics, Russian Academy of Sciences, Kosygin street 4,  
117977 Moscow, V334, RUSSIA

Presles H-N. and Vidal P.

Laboratoire de Combustion et de Detonique, UPR CNRS 9028, ENSMA-Poitiers,  
1 avenue Clement Ader, BP 40109, 86961 Futuroscope-Chasseneuil, France

A model is proposed for interpreting charge diameter effect in ammonium nitrate/aluminium compositions at different content of aluminium and charge density. Based on this model the observed complicated trends can be attributed to variation of ignited fraction of specific surface area of ammonium nitrate. Calculated blast effect of the considered compositions in near-field domain is affected by aluminium particle size.

## INTRODUCTION

Many attempts were done to increase detonation performance of high explosives by addition of aluminium particles but with no significant success.<sup>1</sup> At the same time, introduction of aluminium can easily enhance detonation performance of ammonium nitrate (AN) which is quite weak as an explosive. Available experimental data on effect of charge diameter  $d$  on detonation velocity  $D$  in binary mixtures of ammonium nitrate (AN) with aluminium at porosity ranging from 40 to 50% show that their behaviour is strongly nonideal and that charge density  $\rho_o$  and mass fraction of aluminium  $x_{Al}$  affect these  $D(d)$  dependencies in a non-monotonic way.<sup>2</sup>

Indeed, Figure 1 shows that an increase of  $x_{Al}$  from 0 to 0.02 and then to 0.08 at  $\rho_o$  of about 1050 kg/m<sup>3</sup> (compare experimental curves E6, E4 and E1 respectively) increases detonation velocity  $D$  and decreases critical diameter from approximately 15 cm to 6 cm and then to about 2 cm respectively. However, further increase of aluminium content to 0.12 at the same charge density (curve E3) decreases detonation velocity at fixed diameter and increases critical diameter of detonation to about 4 cm. Increase of charge density from 1050 kg/m<sup>3</sup> to 1170 kg/m<sup>3</sup> at  $x_{Al}=0.08$  decreases detonation velocity (compare E1 and E2). Critical detonation velocity in tested mixtures seems to be about 1500 m/s. Pure AN at smaller density (950 kg/m<sup>3</sup>) has higher detonation velocity than at  $\rho_o=1040$  kg/m<sup>3</sup> (E5 and E6). Detonation velocity in pure AN ranges from about 1000 to 2500 m/s. These regimes are

often considered as low-velocity detonations (LVD). However, clear separation between normal detonation and LVD can be hardly made due to absence of abrupt changes in shape of  $D(d)$  curves.

Leiper and Cooper<sup>3</sup> developed a model for slurry AN/Al mixtures and approved it at fixed 30% porosity and Al content. However, extrapolation to porous mixture and to another range of  $\rho_o$  and  $x_{Al}$  can be quite unreliable.

Here we present a model for porous aluminised explosives which combines such features as local hot spot ignition and growth along with thermodynamic equilibrium equation of state for detonation products and we use this model to interpret available data for AN/Al compositions by gasdynamic numerical simulations of shock-to-detonation transition in tubes of different diameter. All complicated trends can be explained by self-consistent variation of "ignited" part of specific surface area of AN involved in the hot spot growth process. However, the ratio  $\phi$  of this specific surface area to the total one remains a best-fitting parameter of the model. Finally we analyse blast effect of the considered mixtures.

## DESCRIPTION OF THE MODEL

The proposed model treats three-component one-velocity mixture of AN, Al and reaction products and relies on:

a) The gasdynamic conservation equations which take into account porosity of the mixture. The model uses equations of state of these

components at theoretical maximum density. Hence, there is no need to recalibrate equation of state of the mixture when its porosity or composition is modified.

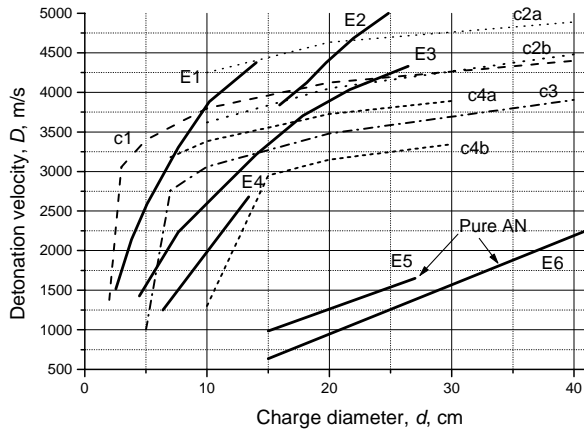


**FIGURE 1. DEPENDENCE OF DETONATION VELOCITY ON CHARGE DIAMETER IN AN/AI MIXTURES LISTED IN TABLE 1. SOLID LINES SHOW EXPERIMENTAL DATA<sup>2</sup>. CALCULATIONS ARE SHOWN BY LINES C1 – C4.**

**TABLE 1. CHARGE DENSITY AND ALUMINIUM CONTENT IN FIGURE 1.**

Exper. #	$\rho_0$ , kg/m <sup>3</sup>	$x_{Al}$
E1	1050	0.08
E2	1170	0.08
E3	1050	0.12
E4	1050	0.02
E5	950	0
E6	1040	0

b) The visco-plastic model of void collapse describing hot spot ignition of porous high explosives.<sup>4</sup> Here, in binary mixtures the situation is more complicated. We assume that pore size is controlled by specific surface and porosity of the charge. Apparently there are voids of different kind: those formed between grains of AN and those contacting Al particles. Ignition of latter voids is considerably delayed in comparison with former voids due to very high thermal activity of metal particles in comparison with AN. For simplicity we look at collapse dynamics and local heating around pores in AN only. To characterize these voids it is convenient to introduce their volume fraction  $\phi$ , which thus will define ignited part of total initial specific surface area. Below  $\phi$  will be used as an empirical parameter of the model.

c) The hot spot growth model, which assumes that contribution of surface burning to the bulk rate of AN decomposition is proportional to a product of

normal burning rate  $r_b = \beta P$ , initial specific surface area  $A_s = 6(\phi_0/d_o)_{AN}$  of AN in the mixture and the afore-mentioned fraction  $\phi$  of ignited part of total initial specific surface area of AN. Here  $\phi_0$  and  $d_o$  are the volume fraction and the mean particle size of AN in the mixture and  $P$  is the local pressure. We remind that specific surface area is one of the most important characteristics of shock sensitivity of heterogeneous explosives since, for example, critical detonation diameter is controlled by their specific surface area, and that shock sensitivity reversal effect observed under decreasing impact pressure is due to reduction of fraction of ignited specific surface area caused by an increase of critical size of hot spots.<sup>5</sup>

d) The metal particle ignition and burning model which, particularly, defines aluminium temperature from the condition of its pressure equilibrium with reaction products and AN. Aluminium ignition occurs when its temperature reaches a threshold temperature. Characteristic time  $\tau_{Al} = Kd_{Al}^2 / x_{ox}^{0.9}$  of oxidation of Al particles by products of AN decomposition is set proportional to a square of mean Al particle diameter  $d_{Al}$  and practically reciprocally proportional to the volume fraction  $x_{ox}$  of species in detonation products capable to oxidize aluminium ( $O_2$ ,  $H_2O$ ,  $CO_2$ , ...).

e) The equilibrium chemistry approach for reaction products. Indeed, reaction progress is controlled by conversion rates of AN and Al, each of which depends on the mean particle size<sup>3</sup>. Therefore, the decomposition process is dominated by mixing and heat conduction rather than by chemical kinetics, which thus is very fast. Hence, composition of detonation products in the course of AN and Al conversion can be described as an equilibrium one and the thermodynamic equilibrium solver, for example<sup>6</sup>, can be used as an equation of state (EOS) of reaction products being in mechanical equilibrium with "solid" AN and Al. As an input, the thermodynamic EOS requires (i) burnt fractions of AN and Al, predicted for example by empirical particle size dependent burning laws, and (ii) specific volume and energy of the mixture given by the solution of gasdynamic equations at every instant of time for every particle trajectory behind the shock. As an output, the thermodynamic EOS returns not only pressure and temperature but also composition of detonation products. Thus, this approach provides correct energetics of the mixture at an arbitrary content of Al, while varying specific surface areas of AN and Al one can vary heat release rate in a wide range between ideal and nonideal explosives.

f) Quasi-one-dimensional description of losses caused by lateral expansion of confining tube. Though this approximation implies that thickness of

confinement wall is small, we shall apply it even for thick tubes since our current purpose is qualitative rather than quantitative analysis of  $D(d)$  dependences resulting from competition between heat release rate in binary mixture and energy losses rate provided by lateral expansion of detonation products and the tube.

Thus, 1D Lagrangian balance equations are read as

$$\frac{\partial u}{\partial t} + (1 - \phi_v)x^v \frac{\partial P}{\partial M} = 0, \quad \phi_v = (a/b)^3$$

$$\partial M / \partial x = Sx^v (1 - \phi_v) / V$$

$$\frac{\partial e}{\partial t} + P \frac{\partial V}{\partial t} = -Q_m \frac{\partial w}{\partial t}, \quad \partial x / \partial t = u$$

$$\frac{\partial w}{\partial t} = \left( \frac{\partial w}{\partial t} \right)_A - w^{2/3} \beta P \phi A_{so} H(\tau - \tau_{ign})$$

$$V = wV_{FM} + (1 - w)V_{DP}$$

$$e = we_{FM} + (1 - w)e_{DP}$$

Here  $u$ ,  $P$ ,  $e$  and  $V$  are the particle velocity, pressure, internal energy and specific volume of the mixture respectively;  $M$  is the Lagrangian mass coordinate,  $v$  is the geometrical factor (0 for plane flow and 2 for the spherical one);  $\phi_v$  is the volume fraction of voids in the binary porous explosive;  $w$  is the mass fraction of fresh explosive,  $(\partial w / \partial t)_A$  is an Arrhenius reaction rate (below we ignore it), while the second term in reaction rate expression corresponds to the surface burn rate;  $H(\tau - \tau_{ign}) = 0$  before ignition and  $H(\tau - \tau_{ign}) = 1$  after ignition takes place at the surface of voids at  $\tau = \tau_{ign}$ ;  $V_{FM} = (1 - x_{Al})V_{AN} + x_{Al}V_{Al}$  is specific volume of the fresh mixture,  $V_{DP}$ ,  $V_{AN}$  and  $V_{Al}$  are specific volumes of detonation products, fresh AN and solid Al,  $e_{FM} = (1 - x_{Al})e_{AN} + x_{Al}e_{Al}$  is the internal energy of the fresh mixture,  $e_{DP}$ ,  $e_{AN}$  and  $e_{Al}$  are internal energies of detonation products, fresh AN and solid aluminium.

Relative cross section of the confining tube,  $S = (r/r_0)^2$ , in quasi-one-dimensional approximation is found from solution of the Newton equation:

$$m \frac{d^2 r}{dt^2} = 2\pi r [P - 2Y \ln(\frac{r_2}{r})]$$

here  $m$  is the specific mass of the tube,  $r_2$  and  $r$  are the outer and inner tube radii ( $r_2^2 - r^2 = const$ ) and  $Y$  is the yield strength of the tube material.

Porosity of the charge  $\phi_v$  depends on the radii

of the hollow cell  $a$  and  $b$  representing the void surrounded by solely AN grains, which were found solving micro-level equations<sup>4</sup> describing void collapse and local heating of AN around the voids. After ignition happens at the void surface along the given particle trajectory behind a shock, the surface burn rate in macroscopic equations is switched on and the void surface temperature is kept constant.

## NUMERICAL SIMULATIONS OF SHOCK-TO-DETONATION TRANSITION

The model was used at first to simulate tests performed by Miyake et al.<sup>7</sup> to study the effect of charge diameter and thickness of 1-m long steel tube on detonation velocity and pressure in pure AN (hence,  $\phi = 1$ ) at density  $\rho_0 = 850 \text{ kg/m}^3$ . Since they reported neither specific surface area of their prills (with a diameter between 1 and 2.8 mm) nor mean void size, we assume that equivalent AN grain size is about 1 mm and then AN specific surface area  $A_{so} = 3 \text{ mm}^{-1}$  (note, however, that only the product  $\beta \phi A_{so}$  is significant for the model). The constant  $\beta$  in the burning law of AN was varied to provide reasonable agreement with observed run distance to detonation and with charge diameter effect (calculated detonation velocity mainly exceeds the experimental one but not larger than by 5%). Best-fitting value of  $\beta$  is  $6 \cdot 10^{-9} \text{ m/s/Pa}$ .

Figure 2 shows calculated dynamics of shock-to-detonation transition in AN/Al mixture at Al mass fraction  $x_{Al} = 0.08$  and  $0.12$  in steel tubes with different diameter at fixed wall thickness  $h_0 = 5 \text{ mm}$ . For simplicity at first we ignore effect of Al on local ignition during void collapse and thus take  $\phi = 1$ . Aluminium particle size is assumed to be  $50 \text{ }\mu\text{m}$ . Detonation is initiated by 66-mm long pellet of PETN. One can see that at  $x_{Al} = const$  the instantaneous shock velocity and final detonation velocity decrease as tube diameter drops (i.e., final detonation velocity in 30-mm diameter tube is about 3000 m/s). Increase of  $x_{Al}$  from 0.08 to 0.12 decreases detonation velocity at fixed values of other control parameters. Also, there is a critical tube diameter below which detonation propagates in irregular LVD mode.

Figure 3A shows profiles of normalised pressure (lower band of the figure), ratio of void radius to its initial value (intermediate band) and normalised temperature at void surface at  $d = 200 \text{ mm}$  and  $h_0 = 5 \text{ mm}$ . Profiles are shown with a time period of  $20 \text{ }\mu\text{s}$ . One can see that pressure profiles have typical triangular shape caused by lateral expansion of detonation products. Void radius behind a shock drops by a factor about 10 resulting in an increase of void surface temperature due to a visco-plastic dissipation of shock energy.

Figure 3B shows for the same conditions profiles of reaction progress in AN and Al. Consumption rate of AN rapidly slows down behind the shock as a result of pressure decrease. The thickness of reaction zone in the quasi-steady detonation wave is quite large and amounts to about 30 mm. Incompleteness of AN conversion in detonation wave (here about 20%) increases as charge diameter is decreased causing respective drop of detonation velocity.

An important advantage of the use of thermodynamic equation of state is a possibility to follow evolution of composition of detonation products in time and in space. Figure 3C and Figure 3D show the number of moles of condensed aluminium oxide and of available oxygen respectively for the same conditions as above.

Figure 3E shows profiles of relative tube radius,  $r/r_0$ . One can see that within the quasi-steady part of the detonation zone the relative expansion of the tube is less than about 50%. Nevertheless, one cannot expect that the oversimplified description of the tube expansion can provide quantitative agreement with experimental charge diameter effect.

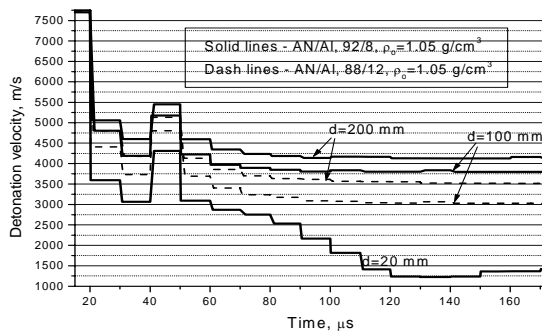


FIGURE 2. SHOCK-TO-DETONATION TRANSITION IN 1-m LONG STEEL TUBE.

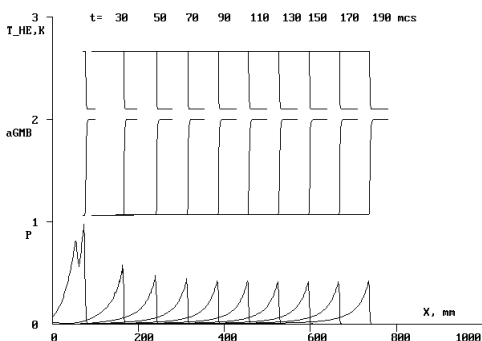


FIGURE 3A. PRESSURE PROFILES (P/140 kbar), DYNAMICS OF VOID COLLAPSE ( $1+a/a_0$ ) AND TEMPERATURE AT VOID SURFACE ( $2+T/3000K$ ) AT  $x_{Al}=0.12$  AND  $\rho_0=1050 \text{ kg/m}^3$ .

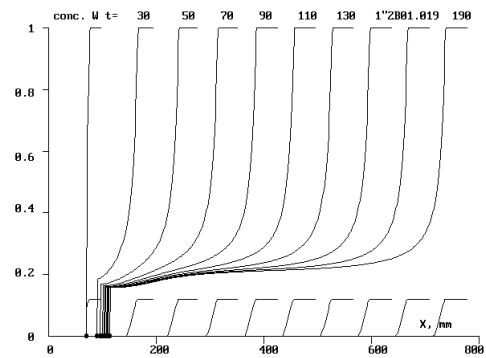


FIGURE 3B. DYNAMICS OF CONSUMPTION OF AMMONIUM NITRATE AND ALUMINIUM.

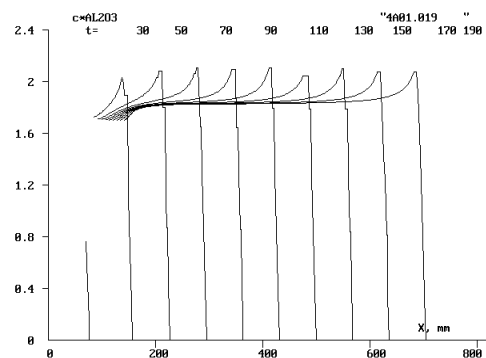


FIGURE 3C. NUMBER OF MOLES OF CONDENSED ALUMINUM OXIDE.

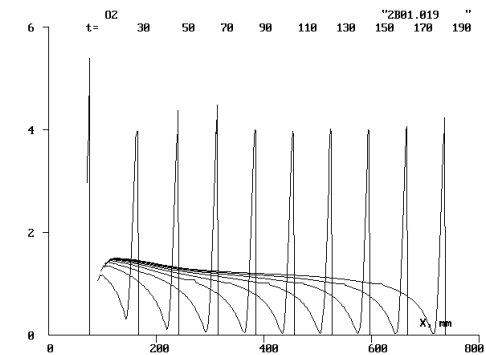


FIGURE 3D. NUMBER OF MOLES OF OXYGEN AT DIFFERENT TIME INSTANTS.

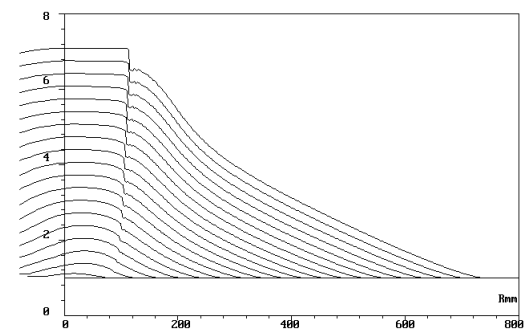
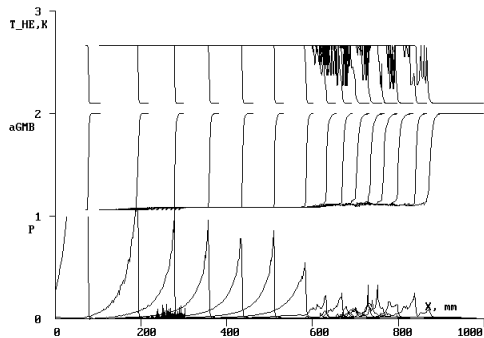
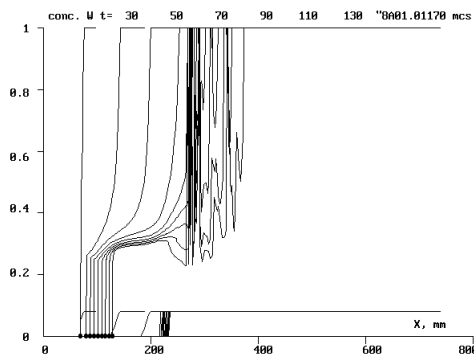


FIGURE 3E. PROFILES OF RELATIVE TUBE RADIUS AT  $t=10, 30, 50, \dots, 190 \mu\text{s}$

Figure 4 shows pressure profiles for low-velocity detonation regime at  $d=20$  mm,  $x_{Al}=0.08$  and  $\rho_o=1050$  kg/m<sup>3</sup>. One can see that initiating shock in contrast to Figure 2 due to stronger lateral expansion fails to provide sufficiently fast void collapse. As a result, void surface temperature becomes too low for local ignition of AN and reaction front separates from the shock front. In this case hot-spot ignition becomes most slow stage. In addition, front of ignition of aluminium particles remains far behind the leading shock, as one can see from Figure 5 obtained for the same conditions.



**FIGURE 4. PROFILES OF PRESSURE (P/3000 kbar), RELATIVE VOID RADIUS ( $1+a/a_0$ ) AND OF VOID SURFACE TEMPERATURE ( $2+T/3000K$ ) IN THE LOW-VELOCITY DETONATION CASE.**



**FIGURE 5. DYNAMICS OF REACTION PROGRESS IN THE LOW-VELOCITY DETONATION CASE.**

#### CHARGE DIAMETER EFFECT

Let us see if the proposed model could help one to understand the general trends manifested by AN/Al mixtures of different density and Al content (Figure 1). The “basic” curve c1 is calculated assuming  $\phi=0.78$  and corresponds to conditions of experimental curve E1 (see Table 1). There is reasonable agreement between c1 and E1 near critical diameter. At larger diameter discrepancy between C1 and E1 becomes more important which could be attributed to oversimplified description of tube expansion and to the fact that we ignore bulk

Arrhenius reaction whose contribution to heat release rate would become more and more important as detonation velocity and pressure grows. Nevertheless, the model reproduces the general character of  $D(d)$  curve.

Let us compare cases 1 and 3 which correspond to  $x_{Al}=0.08$  and  $0.12$  respectively at  $\rho_o=1050$  kg/m<sup>3</sup>. Increase of aluminium content at constant charge density slightly increases void volume fraction (from 0.41 to about 0.42) and slightly decreases AN volume fraction (from 0.56 to 0.53) while total specific surface area of AN decreases from 3.32 mm<sup>-1</sup> to 3.2 mm<sup>-1</sup> (assuming that mean particle size of AN remains the same in both cases). Thus, at the same pressure the mixture E3 should burn only slightly slower than mixture E1 if we assume that  $\phi=0.78$  both for cases 1 and 3. Global heat effect in the case E3 is lower than in the case E1 since the ideal detonation velocity (at infinite charge diameter) is smaller at larger aluminium content (5000 m/s at  $x_{Al}=0.08$  and 4882 m/s  $x_{Al}=0.12$ ). Hence, the “predicted” decrease of heat release rate and detonation velocity at the same charge diameter after transition from case E1 to E3 is quite small. Indeed, the resulting curve c3a is so close to c1 that we did not show it in Figure 1. However, experimental curve E3 strongly differs from E1. Most likely reason is related with our inability to predict the change in parameter  $\phi$ , i.e. in ignited part of specific surface area of AN, after content of aluminium particles was increased by 50%. The curve c3 in Figure 1 was calculated assuming that  $\phi=0.5$  rather than  $\phi=0.78$  used for c1. Then agreement between E3 and c3 becomes acceptable, especially, near critical diameter.

Curves c4a and c4b are calculated for mixture E4 with only 2% of aluminium at  $\phi=0.78$  and  $0.5$  respectively. One can see that better agreement with experimental curve E4 is obtained at larger value of  $\phi$ . Thus, the smaller content of aluminium, the smaller critical hot size and the larger the fraction of “ignited” specific surface area of AN. Simulations of curve E2 corresponding to a larger density of the charge at constant aluminium content show that detonation velocity drops in comparison with E1 due to decrease of available specific surface area and optimum value of  $\phi$  falls between 0.5 and 0.78 (see c2a and c2b).

Thus, varying “ignited” part of specific surface area of AN in the mixture with Al the model allows one to interpret successfully measured  $D(d)$  curves at different values of charge density and aluminium content. It is worth to note two factors in favour of the model. First, the range of variation of  $\phi$  is quite small. Second, trends of these variations can be easily understood from physical point of view.

## SIMULATION OF BLAST EFFECT

Here we apply the proposed model to study the effect of aluminium particles size on propagation of a blast wave resulting from detonation of spherical charge of the mixture AN/Al 70/30 at  $\rho_0=1170 \text{ kg/m}^3$ . As a booster we again use PETN at theoretical maximum density. Mass of the booster is 0.225 kg and its radius is 31.2 mm. Mass of the tested AN/Al mixture is 8.9 kg. External radius of the firing assembly is 122 mm. The booster is initiated at the centre of symmetry ( $R=0$ ) by a point explosion with the energy of 0.15 MJ.

Figure 6 shows pressure profiles during blast wave propagation in the case of fine 1- $\mu\text{m}$  aluminium particles (a solid point on pressure profiles shows position of contact boundary between air and detonation products). Figure 7 compares pressure records at distances  $R=1 \text{ m}$ , 2 m and 4 m from the centre of the charge for aluminium particle size of 1  $\mu\text{m}$  and 50  $\mu\text{m}$ . Figure 8 shows for the same conditions impulse recorded by the same pressure gauges as in Figure 7. Replacement of 1- $\mu\text{m}$  Al particles by coarser 50- $\mu\text{m}$  particles at constant content of aluminium in the mixture decreases detonation parameters within the charge and blast wave velocity, pressure and impulse in the near-field zone. Hence, scaling law relating normalised blast wave overpressure with a dimensionless run distance of the blast wave does not hold in the near-field zone. However, with increase of blast wave run distance the effect of aluminium particle size becomes less and less important. However, in the far-field region the considered 1D model is not valid since it does not take into account mixing of detonation products (and unburned Al particles) with ambient air and corresponding enhancement of blast strength.<sup>8</sup>

The results shown in this section were obtained in the case favourable for rapid detonation build-up due to a high value of ignited specific surface. If more realistic value for ignited specific surface area is used then degree of AN conversion in the detonation wave drops and ignition of aluminium can become rate controlling stage. Results of calculations show that in the considered spherical case only marginal detonations are likely to be initiated in the tested AN/Al 70/30 mixture (however, in larger charges detonation build-up takes place). Overall aluminum consumption is very small (the shock rapidly becomes too weak to ignite aluminum particles). Probably it also means that the assumption on mechanical equilibrium between solid aluminum and AN before aluminum ignition becomes inadequate under these conditions. Incompleteness of AN burning prior to beginning of dissemination stage is above 50%. However such situations are not easy to study with explicit Lagrangian code we have used. Indeed,

expansion of gaseous detonation products normally results in gradual increase of both length of Lagrangian meshes and mean time step controlled by Courant criterion. However, situation becomes dramatically different if some of mixture components remain unburned behind a shock. Length of these meshes with, for example, unburned aluminium always remains much smaller than length of neighbour cells with only gaseous products inside them. This feature strongly limits the time step and makes calculations with explicit schemes quite expensive.

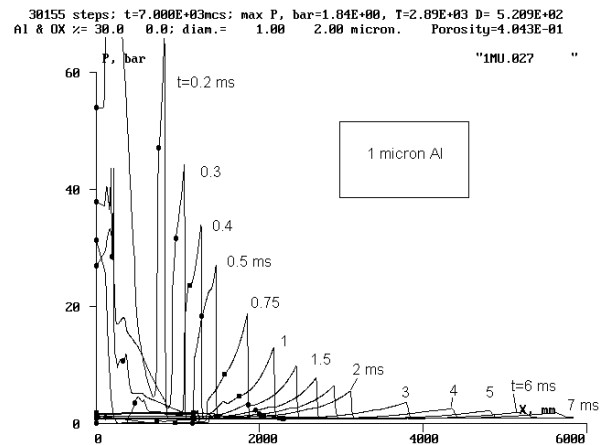


**FIGURE 6. PRESSURE PROFILES AT DIFFERENT INSTANTS OF TIME DURING BLAST WAVE PROPAGATION IN THE CASE OF FINE 1- $\mu\text{m}$  Al PARTICLES**

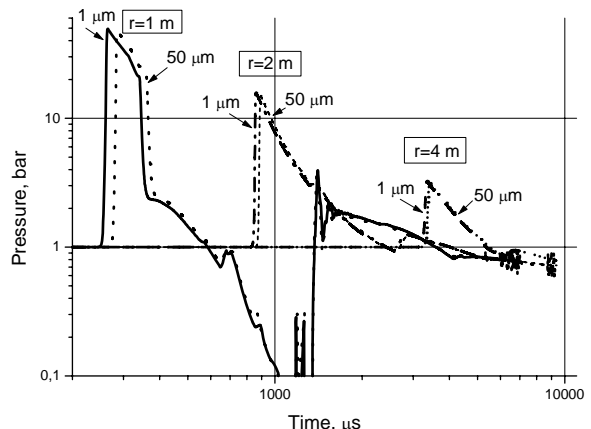


**FIGURE 7. CALCULATED PRESSURE RECORDS AT DISTANCE  $R=1, 2$  AND  $4 \text{ m}$  FROM THE CENTRE OF THE CHARGE FOR 1- AND 50- $\mu\text{m}$  Al PARTICLES.**

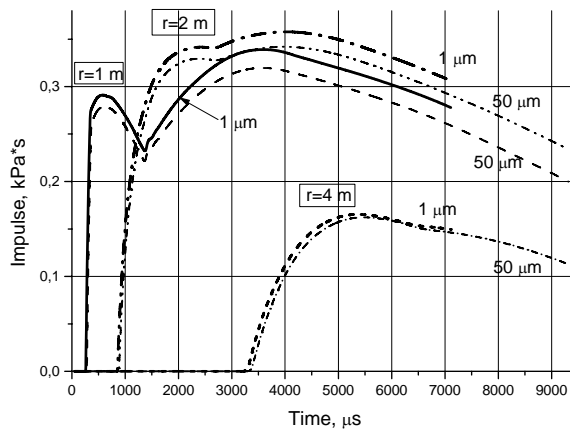


**FIGURE 8. CALCULATED IMPULSE RECORDS AT DISTANCE  $R=1, 2$  AND  $4$  m FROM THE CENTRE OF THE CHARGE FOR 1- AND  $50\text{-}\mu\text{m}$  Al PARTICLES.**

## CONCLUSIONS

By varying “ignited” part of specific surface area of AN in the mixture with Al the proposed model can interpret successfully experimentally observed charge diameter effect at different values of charge density and aluminium content. However, here this “ignited” part of specific surface area is considered as the best-fitting parameter of the model and hence it would be interesting to develop a model for its evaluation. To facilitate such modelling the data on microstructure of binary mixtures are needed.

The model was applied to simulate expansion of detonation products of spherical AN/Al charge. It is shown that variation of aluminum particle size at constant content of aluminum in the mixture affects blast wave amplitude in the near-field zone. In the considered example at realistic value of “ignited” part of specific surface area of AN the model predicts only marginal detonations with nearly 50% degree of AN decomposition behind a shock. Assumption on mechanical equilibrium between solid aluminum and AN before aluminum ignition becomes probably inadequate under these subcritical conditions since aluminum particles do not ignite in the considered example. On another hand, presence of condensed unburned products behind a blast wave results in serious numerical difficulties when applying explicit Lagrangian scheme in gasdynamic modelling.

## REFERENCES

1. Ermolaev B.S., Khasainov B.A., Baudin G., Presles H.-N. (2000) “Behaviour of aluminium in detonation of high explosives. Surprises and interpretations”. Chem. Phys. Reports, Vol. 18 (6), P.1121-1140.
2. “Physics of explosions”. Ed. Stanyukovich. Moscow, Nauka: 1975 (in Russian)
3. Leiper G.A., Cooper J. “Reaction of aluminium and ammonium nitrate in nonideal heterogeneous explosives”. Tenth International Detonation Symposium, ONR 33395-12, 1993, p.267-275.
4. Khasainov B.A., Ermolaev B.S., Presles H.-N. (1993) “Effect of glass microballoons on shock wave sensitivity and detonation critical diameter of condensed explosives”. Tenth International Symposium on Detonation, Office of Naval Research, ONR 33395-12, P. 749-757.
5. Khasainov B.A., Ermolaev B.S., Presles H.-N., Vidal P. (1997) “On the effect of grain size on shock sensitivity of heterogeneous high explosives”. Shock Waves, V. 7, P. 89-105.
6. Imkhovik N.A., Soloviev V.S. Proc. 21-st International Pyrotechnic Seminar (Inst. Chem. Phys. RAS, Moscow, 1995), p.316.
7. Miyake A., A.C. van der Steen, Kodde H.H. “Detonation velocity and pressure of the nonideal explosive ammonium nitrate”. Ninth International Detonation Symposium, NSWC, 1989, p.560-565.
8. Kuhl A.L., Bell J.B., Ferguson R.E., Chien K.-Y., Collins J.P., Lyons M.-L. “Evolution of turbulent fields in explosions”. Proceedings of the Zel’dovich Memorial. International Conference on Combustion, Moscow, 12-17 September, 1994. p.258-260.